Journal of Applied Mechanics and Technical Physics, Vol. 47, No. 5, pp. 643–653, 2006

TWO-DIMENSIONAL PROBLEM OF THE IMPACT OF A VERTICAL WALL ON A LAYER OF A PARTIALLY AERATED LIQUID

A. A. Korobkin

UDC 532.59+539.3+534.12

The two-dimensional unsteady problem of the impact of a vertical wall on a layer of a liquid which is mixed with air near the wall and does not contain air bubbles away from the wall is solved in a linear approximation. The gas–liquid mixture is modeled by a homogeneous, ideal, and weakly compressible medium with a reduced sound velocity dependent on the air concentration in the gas–liquid mixture. Outside the gas–liquid layer, the liquid is considered ideal and incompressible. During the initial stage of the impact, the liquid flow and the hydrodynamic pressure are determined using the linear theory of the potential motion of an inhomogeneous liquid. The dependence of the amplitude of the impact pressure along the wall on the air concentration in the gas–liquid layer and on the thickness of this layer is investigated. For a small relative thickness of the layer, the thin-layer approximation is used. It is shown that the solution of the original problem tends to the approximate solution as the thickness of the layer decreases. It is shown that the presence of the gas–liquid layer leads to wall pressure oscillations. Estimates are obtained for the pressure amplitude and the oscillation period.

Key words: *impact, aerated liquid, thin-layer approximation.*

Introduction. We consider the two-dimensional unsteady problem of the liquid flow caused by sudden motion of a vertical wall. Prior to the beginning of the motion, the liquid occupies a strip $x > 0$, $0 < y < H$ and is at rest. The horizontal line $y = 0$, $x > 0$ corresponds to an even impenetrable bottom of the liquid layer, the line $y = H$, $x > 0$ to its free boundary, and the segment $x = 0$, $0 < y < H$ to the vertical rigid wall (Fig. 1). At a certain time, which is taken as the initial one ($t = 0$), the vertical wall begins to move toward the liquid layer at a constant velocity V. The liquid region consists of two parts: $0 < x < d$ and $x > d$. In the layer adjacent to the wall ($0 < x < d$, $0 < y < H$), the liquid is mixed with air (is aerated) and the density of the gas–liquid mixture is equal to ρ_m. The sound velocity in the aerated liquid is equal to c_m. In the main flow region ($x > d$, $0 < y < H$), the liquid does not contain air bubbles and its motion is described by the ideal incompressible liquid model. The liquid motion in the aerated layer is described using the acoustic approximation, which is formally valid for low impact velocities V. The presence of air bubbles in the aerated layer leads to a decrease in the sound velocity compared to the case of a homogeneous liquid. The nonlinear phenomena due to air bubble oscillations and the dependence of the sound velocity c_m on the hydrodynamic pressure are ignored in the present study. More complete models of wave processes in liquids containing gas bubbles are presented in [1–3].

It is required to determine the hydrodynamic-pressure distribution along the vertical wall during the initial stage of its motion. The duration of the initial stage, in which the pressure reaches a maximum value, depends on wave processes in the gas–liquid layer. If this layer is absent, the incompressible liquid flow established in the main region after the impact is determined with the use of the Sedov impact theory [4], which allows one to find the time integral of the hydrodynamic pressure for small times but not the pressure. The average pressure can be determined from the known integral of the pressure and the duration of the impact stage. However, the concept of the duration of the impact stage is absent in the Sedov impact theory. Therefore, the average pressure

Lavrent'ev Institute of Hydrodynamics, Siberian Division, Russian Academy of Science, Novosibirsk 630090; kaa@hydro.nsc.ru. Translated from Prikladnaya Mekhanika i Tekhnicheskaya Fizika, Vol. 47, No. 5, pp. 34–46, September–October, 2006. Original article submitted November 1, 2005.

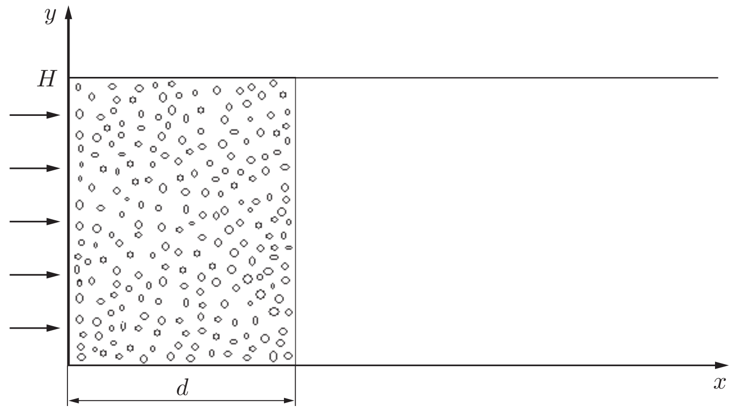

Fig. 1. Impact of the vertical wall on the aerated liquid layer.

is calculated invoking additional hypotheses [5] based on an analysis of experimental data or taking into account acoustic effects. Experimental data have shown that the maximum impact pressures are reached for small times, where the displacements of the wall and liquid particles are smaller than the linear dimension of the liquid region. To calculate the maximum hydrodynamic pressure during impact, one can ignore the shape variation of the flow region in the initial stage, to linearize the equations of motion and the boundary conditions, and to impose the latter on the boundary of the liquid in its initial position. This approximation is standard in impact problems for both the incompressible liquid model and the model of a weakly compressible liquid [5]. In the last case, we obtain the so-called acoustic approximation, where the impact-induced liquid flow is described by a velocity potential that satisfies the wave equation in the flow region, vanishes on the free boundary of the liquid, and satisfies the nonpenetration condition on the solid boundaries of the region and zero initial conditions. In the acoustic approximation, the pressure is calculated using the linearized Cauchy–Lagrange equations. At the time of impact, the pressure is equal to the "hydraulic hammer" pressure: $p = \rho_0 c_0 V$ (ρ_0 is the density of the liquid, c_0 is the sound velocity in a quiescent homogeneous liquid, and V is the impact velocity). For water without air bubbles, $c_0 = 1500$ m/sec and $\rho_0 = 1000$ kg/m^3. Impact at a velocity $V = 3$ m/sec gives rise to a pressure equal to approximately 4.5 MPa. The high pressure is retained until rarefaction waves from the free boundary of the liquid arrive at the point considered. The rarefaction waves, reflecting from the bottom and the free boundary and interacting with the compression waves, create a complex wave pattern of the process. The wall pressure takes both positive and negative values, but the amplitude of the hydrodynamic pressure oscillations decreases with time. To calculate the maximum pressure, it is sufficient to solve the problem only for small times.

If in the flow there are two regions (in the case considered, one of the regions is the aerated layer adjoining the moving vertical wall), the wave pattern of the process becomes even more complex. Before the time $t_1 = d/c_m$, the boundary $x = d$ remains unperturbed and the wall pressure is specified by the quantity $\rho_m c_m V$ everywhere except in a small zone near the free boundary, where the pressure decreases due to the rarefaction wave extending from the free boundary into the depth of the liquid. In the acoustic approximation, the dimension of this zone along the wall is equal to $c_m t$. On the part of the vertical wall where $0 < y < H - c_m t$, the pressure is still equal to the "hydraulic hammer" pressure $\rho_m c_m V$.

At the time t_1, the weak shock wave formed at the moment of the impact reaches the interface $x = d$ between the pure liquid and the liquid containing air bubbles. The interface is free to move, and the weak shock wave is partially reflected from it. The reflected shock wave moves toward the vertical wall and reaches it at the time $2t_1$. For the points located deep enough on the moving vertical wall so that the rarefaction wave from the free boundary has not yet reached them, we have $p = \rho_m c_m V$ at $0 < t < 2t_1$. At the time $2t_1$, the wall pressure increases sharply, and the shock wave is reflected from the wall, then from the interface, etc. Each cycle of such reflections leads to an increase in the wall pressure until the rarefaction wave reaches the bottom of the liquid layer. The above description of the impact of a vertical wall on a liquid with an aerated layer shows that this process differs significantly from the impact on a homogeneous compressible liquid. The presence of the layer leads to an increase in the pressure with time due to repeated reflections of the weak shock wave from the wall and the interface. If the free boundary was absent, the pressure rise would continue for an infinitely long time provided that the wall velocity was constant. The rarefaction wave propagating from the free boundary into the depth of the liquid limits the pressure rise in the layer. Therefore, it is reasonable to use the quantity $T = H/c_m$ as the characteristic time of the process. If the layer is thin ($\varepsilon = d/H \ll 1$), the time required for the acoustic wave to travel a distance equal to one layer thickness is equal to t_1, and $t_1/T = \varepsilon$. In this case, we have two time scales T and t_1, which differ significantly in order of magnitude, which allows averaging to be employed for an asymptotic analysis of the process.

The averaging method was used in [6] to study the action of acoustic waves in liquids on solids coated with a thin compressible layer. In the present work, this method is employed to solve the problem of the impact in the presence of a thin layer of an aerated liquid. An advantage of the method developed in [6] is that the presence of a thin compressible layer is approximately modeled by a special boundary condition on the body surface. This considerably simplifies the problem and, as shown in [6], does not lead to significant errors in the predictions of pressure distributions and amplitudes. In addition, as noted in [6], the thin-layer approximation allows one to reduce the number of parameters of the problem, which is important in planning experiments and interpreting measurement results.

If the thickness of the aerated layer is comparable to the liquid depth, it is necessary to construct a solution of the complete problem, which involves difficulties even when using the acoustic approximation. In this work, this problem is solved using a spectral method to verify the accuracy of the solution obtained in the thin-layer approximation.

The thin-layer approximation allows one to investigate problems with aerated layers of variable thickness and with depth-varying air concentrations in the layer, taking into account nonlinear effects. In the present paper, such problems are not considered.

The problem of the impact of a vertical wall (or its part) on a liquid layer is closely related to the problem of impact of a breaking wave on coastal structures [5]. If the front of a breaking wave approaching a vertical wall becomes almost vertical and foamed, then in the calculation of the hydrodynamic impact load on the structure, it is possible “to reverse” the motion [5] and study the impact of a part of the wall on the liquid in the presence of a thin aerated layer. This indicates that the problem under consideration is timely and important for applications. In applied problems, accounting for the liquid aeration effect in the region of impact on the hydrodynamic load is important, but simple models suitable for engineering calculations are not available. Use is made of nonlinear models for the motion of multiphase media [5]. They contain many parameters and, because of poor understanding and uncertainty of the real processes of wave impact on coastal structures, these models almost always allow one “to choose” these parameters so that numerical results reproduce some of the real phenomena to some extent.

One might expect that simplified models describing the main features of the phenomenon will be more useful for the solution of practical problems. The purpose of the present work is to study one of these models.

Formulation of the Problem. In the acoustic approximation, the liquid flow in the aerated layer in dimensionless variables is described by a velocity potential $\varphi_a(x, y, t)$ that satisfies the equations

$$\frac{\partial^2 \varphi_a}{\partial t^2} = \frac{\partial^2 \varphi_a}{\partial x^2} + \frac{\partial^2 \varphi_a}{\partial y^2} \qquad (t > 0, \quad 0 < y < 1, \quad 0 < x < \varepsilon); \tag{1}$$

$$\frac{\partial \varphi_a}{\partial x} = 1 \qquad (t > 0, \quad 0 < y < 1, \quad x = 0); \tag{2}$$

$$\frac{\partial \varphi_a}{\partial y} = 0 \qquad (t > 0, \quad y = 0, \quad 0 < x < \varepsilon); \tag{3}$$

$$\varphi_a = 0 \qquad (t > 0, \quad y = 1, \quad 0 < x < \varepsilon); \tag{4}$$

$$\varphi_a = \frac{\partial \varphi_a}{\partial t} = 0 \qquad (t = 0). \tag{5}$$

In the main region, where $x > \varepsilon$, the incompressible liquid flow is described by a velocity potential $\varphi_i(x, y, t)$ that satisfies the equations

$$\frac{\partial^2 \varphi_i}{\partial x^2} + \frac{\partial^2 \varphi_i}{\partial y^2} = 0 \qquad (0 < y < 1, \quad x > \varepsilon); \tag{6}$$

$$\varphi_i = 0 \qquad (y = 1, \quad x > \varepsilon); \tag{7}$$

$$\frac{\partial \varphi_i}{\partial y} = 0 \qquad (y = 0, \quad x > \varepsilon); \tag{8}$$

$$\varphi_i \to 0 \qquad (x \to \infty). \tag{9}$$

The pressure $p(x, y, t)$ in the layer is calculated using the linearized Cauchy–Lagrange integral

$$p = -\frac{\partial \varphi_a}{\partial t}. \tag{10}$$

The pressure scale is $\rho_m c_m V$, the length scale is H, the time scale is H/c_m, and the scale of the velocity potentials is VH. The sound velocity c_m in the gas–liquid mixture is calculated by the approximate formula [3]

$$c_m = c_a \sqrt{\frac{\rho_a}{\alpha(1-\alpha)\rho_0}}, \tag{11}$$

where $c_a = 330$ m/sec is the sound velocity in air, $\rho_a = 1.29$ kg/m^3 is the air density, $\rho_0 = 1000$ kg/m^3 is the water density, and α is the volume fraction of air in the gas–liquid layer. We note that $c_m < c_0/10$ for $\alpha(1-\alpha) > 6.24 \cdot 10^{-3}$. Hence, in practically important cases, the sound velocity c_m in the layer is much lower than the sound velocity in the main flow region, which allows an approximate description of the flow in the main region using the ideal incompressible liquid model. The liquid density in the layer ρ_m is calculated by the formula

$$\rho_m = \alpha\rho_a + (1-\alpha)\rho_0. \tag{12}$$

On the boundary between the layer and the main flow region, the continuity conditions for the pressure and the normal component of the liquid-particle velocity should be satisfied. In the linear approximation, these conditions are given by

$$\frac{\partial \varphi_a}{\partial x} = \frac{\partial \varphi_i}{\partial x} \qquad (x = \varepsilon, \quad 0 < y < 1); \tag{13}$$

$$\varphi_i = \gamma\varphi_a \qquad (x = \varepsilon, \quad 0 < y < 1), \tag{14}$$

where $\gamma = \rho_m/\rho_0$. At low air concentration ($\alpha \ll 1$), in (14) it is possible to set $\gamma \approx 1$.

It is required to construct a solution of the problem (1)–(14), to determine the hydrodynamic pressure distribution along the vertical wall $p(0, y, t)$, and to investigate its dependence on the volume fraction of air in the layer.

Thin-Layer Approximation. Following [6], we integrate the wave equation (1) over x from 0 to ε taking into account the boundary conditions (2) and (13). We find

$$\frac{\partial \varphi_i}{\partial x}(\varepsilon, y, t) - 1 = \frac{\partial^2 \bar{\varphi}_a}{\partial t^2} - \frac{\partial^2 \bar{\varphi}_a}{\partial y^2}, \tag{15}$$

where

$$\bar{\varphi}_a(y, t) = \int_0^{\varepsilon} \varphi_a(x, y, t)\, dx. \tag{16}$$

Using the approximation

$$\varphi_a(x, y, t) = \varphi_a(\varepsilon, y, t) + O(\varepsilon)$$

and the conjugation condition (14), we can write (16) in the form

$$\bar{\varphi}_a(y, t) \approx (\varepsilon/\gamma)\varphi_i(\varepsilon, y, t) + O(\varepsilon^2). \tag{17}$$

In the leading-order approximation for $\varepsilon \to 0$, Eqs. (15) and (17) imply that

$$\frac{\partial \varphi_i}{\partial x} = 1 + \frac{\varepsilon}{\gamma}\Big(\frac{\partial^2 \varphi_i}{\partial t^2} - \frac{\partial^2 \varphi_i}{\partial y^2}\Big). \tag{18}$$

We note that in (18) terms with higher derivatives are retained, although they appear with a small factor ε.

Below, equality (18) is considered as a nonclassical boundary condition [6] for the boundary-value problem (6)–(9). The conjugation condition (14) and the initial conditions (5) show that the solution of the problem (6)–(9), (18) should satisfy the initial conditions

$$\varphi_i = \frac{\partial \varphi_i}{\partial t} = 0 \qquad (t \le 0). \tag{19}$$

Condition (18) should be satisfied at the interface $x = \varepsilon$, but a horizontal shift by ε toward the walls does not lead to a change in the form of Eqs. (6)–(9), (18), and (19), which allows the problem to be examined in the region $x > 0$, $0 < y < 1$. This is equivalent to the extension of condition (18) to the vertical wall $x = 0$. Once the velocity potential distribution $\varphi_i(0, y, t)$ on the left boundary of the liquid region is determined, the pressure distribution along the moving vertical wall is found by the formula

$$p(0, y, t) = -\frac{1}{\gamma}\frac{\partial \varphi_i}{\partial t}(0, y, t). \tag{20}$$

The solution of the problem (6)–(9), (18), (19) is sought in the form

$$\varphi_i(x, y, t) = \sum_{k=0}^{\infty} a_k(t)\, \mathrm{e}^{-\lambda_k x} \cos(\lambda_k y), \qquad \lambda_k = \frac{\pi}{2}(2k+1). \tag{21}$$

Representation (21) satisfies Eq. (6), boundary conditions (7) and (8) and the condition at infinity (9). The unknown coefficients $a_k(t)$ are found using boundary condition (18) and initial conditions (19). Substituting (21) into Eqs. (18) and (19) and using the orthogonality property of the system of functions $\{\cos(\lambda_k y)\}_{k=1}^{\infty}$ in the interval $0 < y < 1$, we obtain

$$a_k(t) = -\frac{\gamma v_k}{\varepsilon \omega_k^2}[1 - \cos(\omega_k t)], \qquad \omega_k^2 = \lambda_k\Big(\lambda_k + \frac{\gamma}{\varepsilon}\Big); \tag{22}$$

$$\frac{\partial a_k}{\partial t} = -\frac{\gamma v_k}{\varepsilon \omega_k} \sin(\omega_k t). \tag{23}$$

Here v_k are the coefficients in the expansion of the impact velocity distribution over the wall height in the system of functions $\{\cos(\lambda_k y)\}_{k=1}^{\infty}$:

$$1 = \sum_{k=0}^{\infty} v_k \cos(\lambda_k y), \qquad v_k = 2\frac{(-1)^k}{\lambda_k}. \tag{24}$$

If the impact velocity (2) varies along the wall, the condition should be replaced by the condition

$$\frac{\partial \varphi_a}{\partial x} = f(y) \qquad (t > 0, \quad 0 < y < 1, \quad x = 0),$$

where the function $f(y)$ describes the impact velocity distribution over the wall height. The remaining formulas remain unchanged, except for expansion (24), which should be replaced by the relation

$$f(y) = \sum_{k=0}^{\infty} v_k \cos(\lambda_k y), \qquad v_k = 2\int_0^1 f(y)\cos(\lambda_k y)\, dy. \tag{25}$$

Formulas (20)–(25) allow the required hydrodynamic pressure distribution along the vertical wall to be written as

$$p(0, y, t) = \frac{1}{\varepsilon}\sum_{k=0}^{\infty} \frac{v_k}{\omega_k} \sin(\omega_k t)\cos(\lambda_k y). \tag{26}$$

Because formula (26) was derived ignoring variations of the unknown functions on spatial and time scales of order $O(\varepsilon)$ for small ε in dimensionless variables, it is reasonable to define the average pressure as

$$\langle p \rangle(y, t) = \frac{1}{\varepsilon^2}\int_{y-\varepsilon/2}^{y+\varepsilon/2}\int_{t-\varepsilon/2}^{t+\varepsilon/2} p(0, y_0, t_0)\, dt_0\, dy_0.$$

The formula for the average pressure has the form (26), where each term is multiplied by the coefficient

$$S_k(\varepsilon) = \frac{\sin(\lambda_k \varepsilon/2)}{\lambda_k \varepsilon/2}\,\frac{\sin(\omega_k \varepsilon/2)}{\omega_k \varepsilon/2}.$$

Solution of the Original Problem. If the thickness of the aerated layer is comparable to the liquid depth, it is required to construct a solution of the problem (1)–(14) and to compare it with the solution obtained using the thin-layer approximation. In the region of the layer, the velocity potential is sought in the form

$$\varphi_a(x,y,t) = \sum_{k=0}^{\infty} \varphi_a^{(k)}(x,t)\cos(\lambda_k y) \qquad (0 < x < \varepsilon), \tag{27}$$

and in the main region, it is sought in the form

$$\varphi_i(x,y,t) = \sum_{k=0}^{\infty} b_k(t)\,\mathrm{e}^{-\lambda_k(x-\varepsilon)}\cos(\lambda_k y) \qquad (x > \varepsilon). \tag{28}$$

The coefficients $\varphi_a^{(k)}(x,t)$ satisfy the equation

$$\frac{\partial^2 \varphi_a^{(k)}}{\partial t^2} = \frac{\partial^2 \varphi_a^{(k)}}{\partial x^2} - \lambda_k^2 \varphi_a^{(k)} \qquad (0 < x < \varepsilon, \quad t > 0), \tag{29}$$

the boundary conditions

$$\frac{\partial \varphi_a^{(k)}}{\partial x} = v_k \qquad (x = 0, \quad t > 0); \tag{30}$$

$$b_k(t) = \gamma \varphi_a^{(k)}(\varepsilon,t), \qquad \frac{\partial \varphi_a^{(k)}}{\partial x}(\varepsilon,t) = -\lambda_k b_k(t), \tag{31}$$

and the initial conditions

$$\varphi_a^{(k)} = \frac{\partial \varphi_a^{(k)}}{\partial t} = 0 \qquad (t < 0). \tag{32}$$

Conditions (31) at the interface $x = \varepsilon$ imply that

$$\frac{\partial \varphi_a^{(k)}}{\partial x} + \gamma\lambda_k \varphi_a^{(k)} = 0 \qquad (x = \varepsilon, \quad t > 0). \tag{33}$$

The initial-boundary-value problem (29), (30), (32), (33) is considered separately from the problem in the main flow region. The coefficients $b_k(t)$ of expansion (28) are calculated after the solution of this problem using formulas (31). The pressure $p(0,y,t)$ along the wall is calculated by formula (10). Taking into account expansion (27), we have

$$p(x,y,t) = \sum_{k=0}^{\infty} p_k(x,t)\cos(\lambda_k y); \tag{34}$$

$$p_k(x,t) = -\frac{\partial \varphi_a^{(k)}}{\partial t}(x,t). \tag{35}$$

The images of the Laplace transform of the functions $\varphi_a^{(k)}(x,t)$ and $p_k(x,t)$ over t will be denoted by $\phi_k(x,s)$ and $q_k(x,s)$, where s is the Laplace transform parameter. Equations (29)–(33) lead to the boundary-value problem for the new unknown function $\phi_k(x,s)$:

$$\begin{gathered} \frac{\partial^2 \phi_k}{\partial x^2} = (s^2 + \lambda_k^2)\phi_k \qquad (0 < x < \varepsilon), \\ \frac{\partial \phi_k}{\partial x} = \frac{v_k}{s} \qquad (x = 0), \\ \frac{\partial \phi_k}{\partial x} + \gamma\lambda_k\phi_k = 0 \qquad (x = \varepsilon), \\ q_k(x,s) = -s\phi_k(x,s). \end{gathered} \tag{36}$$

The solution of the boundary-value problem (36) has the form

$$\phi_k(x,s) = \frac{v_k}{s}\frac{1}{\sqrt{s^2+\lambda_k^2}}\sinh\left(\sqrt{s^2+\lambda_k^2}\,x\right) + D_k(s)\cosh\left(\sqrt{s^2+\lambda_k^2}\,x\right).$$

This representation of the solution satisfies the differential equation and the boundary condition at $x = 0$. From the boundary condition at $x = \varepsilon$, we obtain the coefficient $D_k(s)$:

$$D_k(s) = -\frac{v_k}{s}\,\frac{\cosh\,(\zeta\varepsilon) + \gamma\lambda_k \sinh\,(\zeta\varepsilon)/\zeta}{\zeta \sinh\,(\zeta\varepsilon) + \gamma\lambda_k \cosh\,(\zeta\varepsilon)}, \qquad \zeta = \sqrt{s^2 + \lambda_k^2}.$$

Using the expression $\phi_k(0, s) = D(s)$ and the equality $q_k(0, s) = -sD(s)$, which follows from (35), for the image of the Laplace transform of the coefficients $p_k(0, t)$ in the expansion of the pressure (34), we obtain the formula

$$q_k(0, s) = v_k\,\frac{\cosh\,(\zeta\varepsilon) + \gamma\lambda_k \sinh\,(\zeta\varepsilon)/\zeta}{\zeta \sinh\,(\zeta\varepsilon) + \gamma\lambda_k \cosh\,(\zeta\varepsilon)}. \tag{37}$$

Function (37) does not have branching points. The only singularities of this function are the poles on the imaginary axis $\zeta_{nk} = i\mu_{nk}/\varepsilon$ $(n \geq 1)$, where the real-valued numbers μ_{nk} satisfy the equation

$$\mu_{nk} \tan\,\mu_{nk} = \gamma\varepsilon\lambda_k,$$

and $\mu_{nk} = \pi(n-1) + \Delta_{nk}$, $0 < \Delta_{nk} < \pi/2$, and $\Delta_{nk} \to +0$ as $n \to \infty$. We have the equation

$$\tan\,\Delta_{nk} = \frac{\gamma\varepsilon\lambda_k}{\pi(n-1) + \Delta_{nk}}, \tag{38}$$

which is solved by an iterative method. Thus, $\Delta_{nk} = O(1/n)$ as $n \to \infty$.

The positions of the poles $s = \pm i\omega_{nk}$ of function (37) are determined from the equation $i\mu_{nk}/\varepsilon = \sqrt{\lambda_k^2 - \omega_{nk}^2}$, whence it follows that

$$\omega_{nk} = \sqrt{\mu_{nk}^2/\varepsilon^2 + \lambda_k^2}.$$

The inversion of the formula (37) is based on the residues theorem

$$p_k(0, t) = \sum_{n=1}^{\infty} \Big\{\mathrm{res}\,[\mathrm{e}^{st}\,q_k(0, s), +i\omega_{nk}] + \mathrm{res}\,[\mathrm{e}^{st}\,q_k(0, s), -i\omega_{nk}]\Big\}$$

$$= \frac{v_k}{\varepsilon}\sum_{n=1}^{\infty}\frac{1}{i\omega_{nk}}\,\frac{\mu_{nk}^2 + (\varepsilon\gamma\lambda_k)^2}{\varepsilon\gamma\lambda_k(1 + \varepsilon\gamma\lambda_k) + \mu_{nk}^2}\,(\mathrm{e}^{i\omega_{nk}t} - \mathrm{e}^{-i\omega_{nk}t})$$

$$= \frac{2}{\varepsilon}\,v_k \sum_{n=1}^{\infty} \frac{\mu_{nk}^2 + (\varepsilon\gamma\lambda_k)^2}{\mu_{nk}^2 + \varepsilon\gamma\lambda_k(1 + \varepsilon\gamma\lambda_k)}\,\frac{\sin\,(\omega_{nk}t)}{\omega_{nk}}. \tag{39}$$

Averaging the dimensionless pressure distribution (34), (39) over the time interval τ and on the vertical coordinate y with the length of the averaging interval h, we obtain the following formula for the averaged wall pressure:

$$\langle p\rangle(0, y, t) = \sum_{k=0}^{\infty}\langle p_k\rangle(0, t)\cos\,(\lambda_k y)\,\frac{\sin\,(\lambda_k h/2)}{\lambda_k h/2},$$

$$\langle p_k\rangle(0, t) = \frac{2}{\varepsilon}\,v_k \sum_{n=1}^{\infty} E_{nk}\,\frac{\sin\,(\omega_{nk}t)}{\omega_{nk}}\,\frac{\sin(\omega_{nk}\tau/2)}{\omega_{nk}\tau/2},$$

$$E_{nk} = 1 - \frac{\varepsilon\gamma\lambda_k}{\mu_{nk}^2 + \varepsilon\gamma\lambda_k(1 + \varepsilon\gamma\lambda_k)}.$$

Asymptotic Analysis of the Solutions Constructed. For small ε and finite n and k, formula (38) implies the relations

$$\mu_{1k} = \sqrt{\varepsilon\gamma\lambda_k}\,[1 + O(\varepsilon\gamma\lambda_k)], \qquad \mu_{nk} = \pi(n-1) + O(\varepsilon\gamma\lambda_k) \quad (n \geq 2),$$

$$\omega_{1k} = \sqrt{\frac{\gamma}{\varepsilon}\,\lambda_k[1 + O(\varepsilon\gamma\lambda_k)] + \lambda_k^2} = O\Big(\frac{1}{\sqrt{\varepsilon}}\Big), \qquad \omega_{nk} = O\Big(\frac{1}{\varepsilon}\Big) \quad (n \geq 2).$$

The obtained asymptotic formulas show that for $\varepsilon \to 0$, the term of order $O(1/\sqrt{\varepsilon})$ with number $n = 1$ makes the main contribution to the sum (39). The remaining terms make a contribution of order $O(1)$. Separating the first term in (39) and passing to the limit as $\varepsilon \to 0$ and $\varepsilon\lambda_k = O(1)$, we obtain

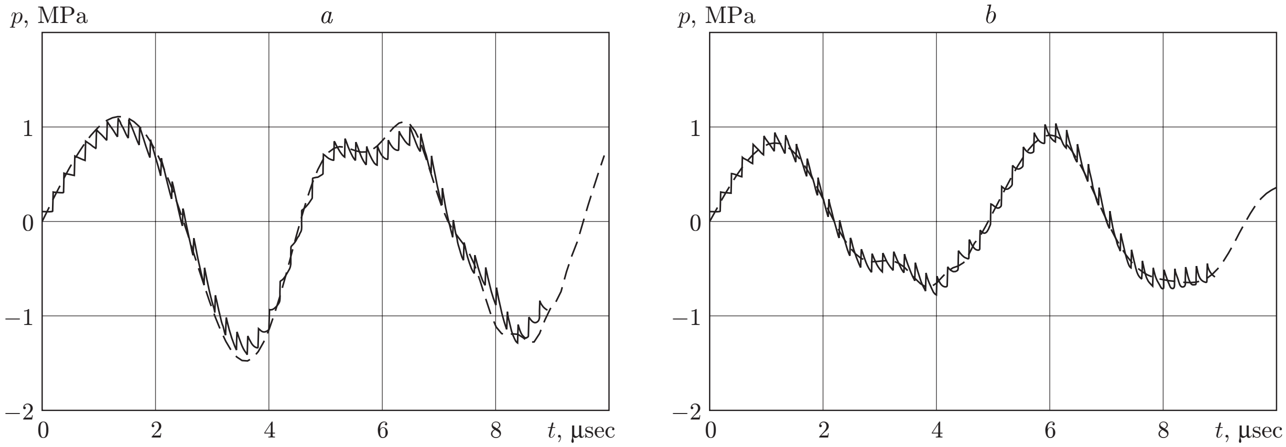

Fig. 2. Impact pressure on the bottom (a) and in the middle of the wall (b) versus time for $d = 1$ cm and $\alpha = 1\%$: the solid curve is calculated for the complete model, and the dashed curve is calculated in the thin-layer approximation.

$$E_{1k} \to \frac{1}{2}, \qquad \omega_{1k}^2 \to \omega_k^2 = \lambda_k^2\Big(1 + \frac{\gamma}{\varepsilon\lambda_k}\Big), \qquad \varepsilon p_k(0,t) \to v_k\,\frac{\sin(\omega_k t)}{\omega_k}.$$

The above asymptotic formulas show that as $\varepsilon \to 0$, the pressure distribution (34) obtained for the complete model reduces to the pressure distribution (26) obtained in the thin-layer approximation.

For small times $t \ll 1$, the wall pressure distribution can be obtained in the form of a series in powers of t by solving problem (6)–(9), (18), (19):

$$p(0,y,t) = \frac{1}{\varepsilon}\Big(t + \frac{1}{6\varepsilon}\,g(y)t^3 + O(t^5)\Big), \quad g(y) = -\frac{1}{2}\Big(\frac{1}{\sin[\pi(1+y)/2]} + \frac{1}{\sin[\pi(1-y)/2]}\Big).$$

The obtained asymptotic solution is not valid near the free boundary. At the bottom point of the wall at $y = 0$, where maximum impact pressures are expected, we have

$$p(0,0,t) = \frac{1}{\varepsilon}\Big(t - \frac{t^3}{6\varepsilon} + O(t^5)\Big).$$

The maximum pressure is reached at $t_{\max} = \sqrt{2\varepsilon}$ and is equal to $p_{\max} = (2\sqrt{2}/3)\varepsilon^{-1/2}$. In the dimensional variables, we find

$$p'_{\max} = \frac{2\sqrt{2}}{3}\,\rho_m c_m V\sqrt{\frac{H}{d}}, \qquad t'_{\max} = \sqrt{2}\,\frac{\sqrt{dH}}{c_m}. \tag{40}$$

The obtained asymptotic estimates of the maximum pressure on the bottom of the liquid layer and the time of its attainment show that the maximum pressure far exceeds the "hydraulic hammer" pressure and is reached well before the rarefaction wave reaches the bottom of the layer. Hence, one of the factors limiting the pressure rise in the gas–liquid layer due to a constant-velocity impact on it is the presence of the interface between the gas–liquid layer and the incompressible homogeneous liquid. This conclusion also follows from numerical calculations by formulas (26) and (34).

Numerical Results. The pressure evolution at various points of the moving wall were calculated by formulas (26) and (34) without averaging over the space and time variables. We note that these formulas gives the "impact" component of the total pressure, to which one needs to add the atmospheric pressure to obtain the total pressure. In the linear model, the pressure is proportional to the impact velocity, which in the calculations was set equal to 1 m/sec, and the thickness of the liquid layer is 1 m.

Figure 2 shows the variation in the impact pressure on the bottom and in the middle of the wall for an aerated layer thickness $d = 1$ cm and $\alpha = 1\%$. It is evident that the thin-layer approximation adequately describes the pressure evolution, except for the high-frequency pressure oscillations due to the repeated reflection of the weak shock wave from the interface and the wall. As the air concentration in the gas–liquid layer increases, the pressure decreases (Fig. 3). The dependences of the maximum and minimum pressures on the volume fraction of air in the

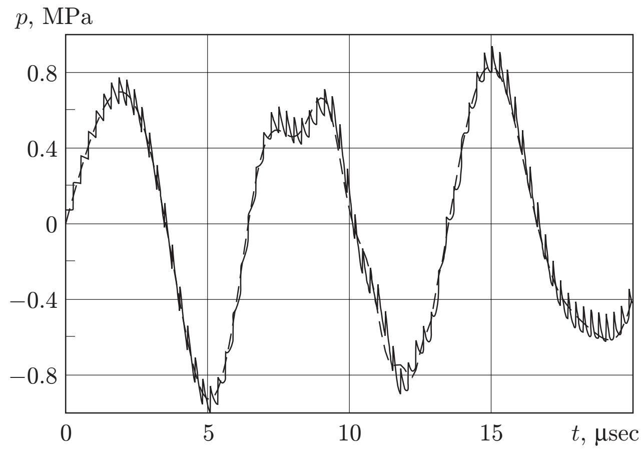

Fig. 3. Impact pressure on the bottom versus time for $d = 1$ cm and $\alpha = 2\%$ (notation the same as in Fig. 2).

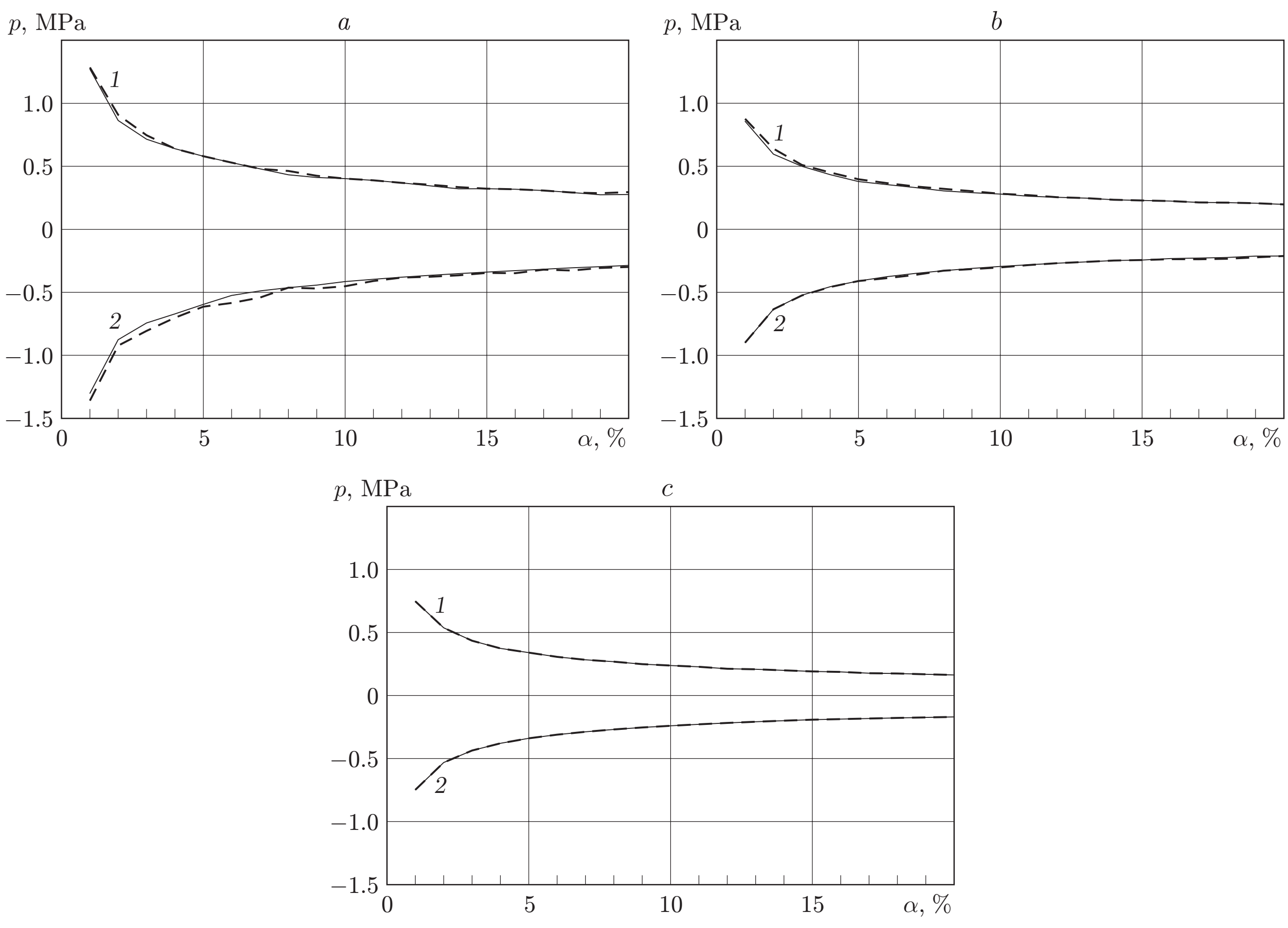

Fig. 4. Maximum wall pressures (curves 1) and minimum wall pressures (curves 2) versus volume fraction of air in the layer for $d = 1$ (a), 2 (b), and 3 cm (c); the solid curve is calculated for the interval $0 < t < 50$; the dashed curve refers to the first peaks of impact pressure on the bottom.

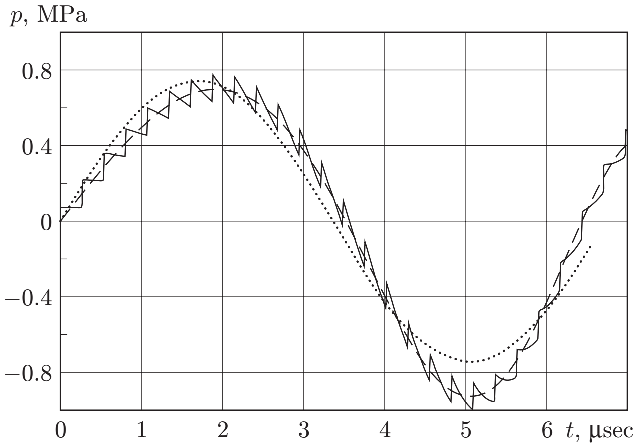

Fig. 5. Impact pressures on the bottom for $d = 1$ cm and $\alpha = 2\%$: the solid curve is calculated by formulas (34) and (39), the dashed curve by formula (26), and the dotted curve by formula (26) with retention of only the first term with number $k = 0$.

layer are shown on Fig. 4. It is evident that for $\alpha > 7\%$, the maximum and minimum pressures vary slightly and their amplitudes decrease with increasing thickness of the layer. The solid curves show the pressure maxima and minima that are reached in the time interval $0 < t < 50$; in each time step, the pressure is calculated at ten points on the wall. The dashed curves show the first pressure peaks on the bottom. The result obtained confirms the assumption that the maximum pressure is reached on the bottom immediately after the impact, and subsequently, it oscillates.

Figure 5 shows impact pressures on the bottom for $d = 1$ cm and $\alpha = 2\%$ obtained by three methods: using formulas (34) and (39) (solid curve), formula (26) (dashed curve), and formula (26), in which only the first term with number $k = 0$ was retained (dotted curve). It is evident that the first term in formula (26) adequately describes the time dependence of the pressure for small times and can be used for tentative estimations of the maximum hydrodynamic pressure during impact and the time of its attainment. Retaining only the first term in (26), we obtain the following estimates:

$$p'_{\max} = \frac{4\sqrt{2}}{\pi^{3/2}}\,\rho_m c_m V \sqrt{\frac{H}{d}}, \qquad t'_{\max} = \sqrt{\frac{\pi}{2}}\,\frac{\sqrt{dH}}{c_m}. \tag{41}$$

A comparison of the asymptotic estimate of the maximum pressure (40) and estimate (41) obtained by numerical analysis shows that they differ by less than 7%.

Conclusions. For the impact of a breaking wave on protective coastal structures, a simplified model taking into account the aeration of the wave head in the region of the impact was constructed and studied. In the aerated part of the liquid, the pressure distribution was described in the acoustic approximation, and in the main flow region, it was described using the ideal incompressible liquid model. The solution of the complete linear problem and the solution of the problem in the thin-layer approximation were constructed and investigated. It was shown that as the thickness of the aerated layer decreases, the complete solution reduces to the approximate solution constructed. The maximum impact pressure as a function of the air concentration in the layer was determined. Simple formulas for estimating the first maximum of impact pressure and the time of its attainment were obtained.

We note that in practice, the thickness of the aerated layer and the air concentration in it is difficult to determine with proper accuracy. The model proposed in this paper remains complex since it contains the indicated parameters. However, the product $p'_{\max}t'_{\max}$ depends weakly on these parameters. Using estimates (41) and the approximation $\rho_m \approx \rho_0$, we obtain $p'_{\max}t'_{\max} \approx (4/\pi)\rho_0 VH$. The right side of this expression contains only the wave velocity and the wave height, which can be measured sufficiently accurately in practice.

This work was performed within the project of the Russian Academy of Sciences No. 5 “Impact on the Free Boundary of a Gas–Liquid Medium” and supported by the Foundation “Leading Scientific Schools” (Grant No. NSh 902.2003.01).

REFERENCES

1. R. I. Nigmatulin, *Dynamics of Multiphase Media*, Hemisphere, New York (1991).
2. V. K. Kedrinskii, *Hydrodynamics of Explosion: Experiment and Models* [in Russian], Izd. Sib. Otd. Ross. Akad. Nauk, Novosibirsk (2000).
3. C. E. Brennen, *Fundamentals of Multiphase Flow*, Cambridge Univ. Press, Cambridge (2005).
4. L. I. Sedov, *Two-Dimensional Problems of Hydrodynamics and Aerodynamics* [in Russian], Gostekhteoretizdat, (1950).
5. D. H. Peregrine, "Water-wave impact on walls," *Annu. Rev. Fluid Mech.*, **35**, 23–43 (2003).
6. L. E. Pekurovskii, V. B. Poruchikov, and Yu. A. Sozonenko, *Interaction of Waves with Bodies* (*Nonclassical Boundary Conditions*) [in Russian], Izd. Mosk. Gos. Univ., Moscow (1990).